Engineering Science and Technology, an International Journal xxx (xxxx) xxx

HOSTED BY

ELSEVIER

Contents lists available at ScienceDirect

Engineering Science and Technology, an International Journal

journal homepage: www.elsevier.com/locate/jestch

Full Length Article

Generating temperature cycle profile from in-situ climatic condition for accurate prediction of thermo-mechanical degradation of c-Si photovoltaic module

Frank K.A. Nyarko [a,*], G. Takyi [a], Emeka H. Amalu [b], Muyiwa S. Adaramola [c]

[a] Department of Mechanical Engineering, College of Engineering, Kwame Nkrumah University of Science and Technology Kumasi, Ghana
[b] Department of Engineering, School of Science and Engineering and Design, Teesside University, Middlesbrough, Tees Valley TS1 3BA, UK
[c] Faculty of Environmental Sciences and Natural Resource Management, Norwegian University of Life Science, As, Norway

ARTICLE INFO

Article history:
Received 3 August 2018
Revised 17 December 2018
Accepted 18 December 2018
Available online xxxx

Keywords:
Temperature cycling
Ramp rates
Temperature gradient
Accelerated Thermal Cycling (ATC)
Co-efficient of Thermal Expansion (CTE)
Rainflow counting
In-situ data generation

ABSTRACT

The use of climate specific temperature-cycling profile is critical to precisely quantifying the degradation rate and accurately determining the service fatigue life of crystalline silicon photovoltaic (c-Si PV) module operating in various climates. A reliable in-situ outdoor weathering database is pivotal to generating the required climate specific temperature cycle profile. This research utilizes high-resolution data obtained at five minutes interval from installed c-Si PV modules to generate a temperature cycle profile that is representative of a test site in sub-Saharan Africa climate. The study collected a three-year data from 2012 to 2014 on weathering of c-Si PV module located at College of Engineering, KNUST Ghana. The data site is on latitude 6° 40′ N and longitude 1° 37′ W at an elevation of 250 m above sea level. Analysis of the data on temperature variation and thermally induced stresses demonstrates that the region has a profile with a ramp rate of 8.996 °C/h, a hot dwell time of 228 min, cold dwell time of 369 min. Maximum and minimum module temperatures of 58.9 °C and 23.7 °C, respectively; and a cycle time of 86400 s. Comparison with the IEC 61215 standards for terrestrial PV modules qualification reveals percentage changes of – 91%, 2180%, 3590%, 747% for the ramp rate, dwell (hot and cold) and cycle times, respectively. The generated in-situ temperature cycle profile predicts to qualify accurately, c-Si PV modules operating in the sub-Saharan African test site. The systematic technique employed in this study to generate the in-situ temperature cycle profile would be useful to the thermo-mechanical reliability research community. In addition, photovoltaic design and manufacturing engineers may harness the information to create climate specific robust c-Si PV module.

1. Introduction

The economics of the PV systems are based on their ability to deliver the rated power over their expected service lifetime, irrespective of their capacity [1]. The results from field studies conducted by a number of researchers have shown that outdoor degradation rates are much higher than expected. Rosenthal et al. and Sørensen et al. [2,3] reported that installed modules experience annual power degradation rates of about 0.5–10%. In the tropical climate of eastern Nigeria, *Ike* [4] studied the variation of power output of field PV modules over a duration of the ambient temperature. The setup was mounted on an iron roof at an angle equivalent to the local latitude (site location; 6° 10′ 0″ North, 7° 4′ 0″ East). The author reported that power output degrades with an increase in ambient temperatures. Walsh et al. [5] conducted a similar study involving the Singapore tropical climate on a rooftop at the National University of Singapore (site location; 1° 17′ 44″ N, 103° 46′ 36″ E). One significant finding from the study revealed that high year-round humidity is the greatest threat to the PV module durability. In addition, they observed that high ambient temperatures and highly diffuse light conditions have some negative effects on PV module output power. Furthermore, Ogbomo et al. [6] studied the effects of operating temperature on the degradation of solder joints in crystalline silicon photovoltaic modules. One of the key findings from their study shows that solder degradation increase with every 1 °C cell temperature rise from Standard Test Conditions (STC). They further observed module fatigue life, L

* Corresponding author.
E-mail addresses: fnyarko.coe@knust.edu.gh (F.K.A. Nyarko), gtakyi.soe@knust.edu.gh (G. Takyi), E.Amalu@tees.ac.uk (E.H. Amalu).

Peer review under responsibility of Karabuk University.

https://doi.org/10.1016/j.jestch.2018.12.007
2215-0986/

(in years) decay, according to the power function 'L = $721.48T^{-1.343}$, where T is the ambient temperature. McCormick and Suehrcke [7] on the other hand, investigated the effect of the intermittency of solar radiation on the performance of photovoltaic (PV) systems with battery storage. Consequently, they developed a model that simulated system energy flows with one-minute and hourly solar radiation values. Additionally, the researchers found that cloudy conditions caused significant fluctuations in system currents. Several researchers have also conducted related studies on the effects of temperature and irradiance on solar PV performance [8–12].

A number of factors cause PV modules installed in the field to degrade. Exposure to a range of cyclic temperatures coupled with operations in elevated temperatures induces cyclic thermo-mechanical stresses in the solder joint interconnections in the crystalline silicon photovoltaic (c-Si PV) modules. In addition, operations under a range of operating currents and voltages and the band-gap of ultraviolet (UV) light incident on the PV play a significant role in accumulating power degradation in PV modules. Huge variations in weather conditions also significantly increase the degradation rate. The contributions of these factors on the degradation of c-Si PV modules operating in sub-Saharan climate is critical. Makenzi et al. [13] demonstrated in their report that the degradation and failure mechanisms of PV modules are location dependent.

Degradation of PV modules is by various failure mechanisms including:

- Corrosion of solder joints and electrical contacts by diffusion of water vapour into the encapsulated cell.
- Induced thermo-mechanical stress on solder joints occasioned by ambient temperature cycling.
- Intermetallic (IMC) growth in solder interconnects caused by long-term exposure to high ambient temperature (thermal soaking and aging).
- Presence of micro-cracks caused by vibrations resulting from hailstorms and high winds.

The development of indoor tests that have the ability to predict real outdoor conditions accurately is quite challenging. A number of research findings suggest various methods which include expanding on the certification procedures outlined in IEC 61215 thermal cycling test (TC 200) by increasing the number of cycles, increasing the temperature range or ramp rates [14]. Other studies have also used field data for PV reliability prediction. For instance, Cuddalorepatta et al. [15] in their study of the durability of Pb-free solder between copper interconnect and silicon in PV cells used a field condition with a temperature range between 63 °C and 17 °C from a data provided from a sponsoring company. Park et al. [16] on the other hand used field data with a cycle time of 24 h: 23–67 °C; 390 min ramp up and 330 min ramp down; 2 h dwell in high temperature and 10 h in low temperature to estimate the degradation rate of multi-crystalline silicon. However, the authors did not demonstrate how they generated the temperature cycle parameters in their respective studies.

An improvement of the current IEC 61215 (TC 200) temperature profile that would lead to improvement in the prediction of module long-term outdoor reliability remains a research task. Solar PV modules experience direct exposure to sunlight in an alternating day/night cycles in service. Furthermore, the exposure induces thermo-mechanical stress on the solder interconnection joints within the module. Fig. 1 presents the architecture of a conventional c-Si PV cell interconnection.

The conventional cell-to-cell interconnection architecture of c-Si PV modules involves connecting solder-coated copper (Cu) ribbons in a series arrangement. The ribbons connect the silver (Ag) electrodes deposited in the silicon crystal via solder bonds. These materials forming the interconnections of the module have different co-efficient of thermal expansion (CTE). Park et al. [16] explains that the variation in the CTE of constituent materials bonded together to form the module induces the thermo-mechanical stress. Consequently, the load effects culminate in the initiation and development of fatigue cracks in the solder interconnection. Fatigue cracks in the joints increase module series resistance losses (Rs) and causes an overall drop in PV output power [17]. Gonzalez et al. [18] reported that the higher CTE mismatch between glass and cells may cause the cells to separate from the assembly. Furthermore, high daily module temperatures aggravate the situation.

Generally, an increase in temperature induces tensile stress in materials and thus in the interconnection. Decrease in temperatures lower than the stress free temperature condition at night

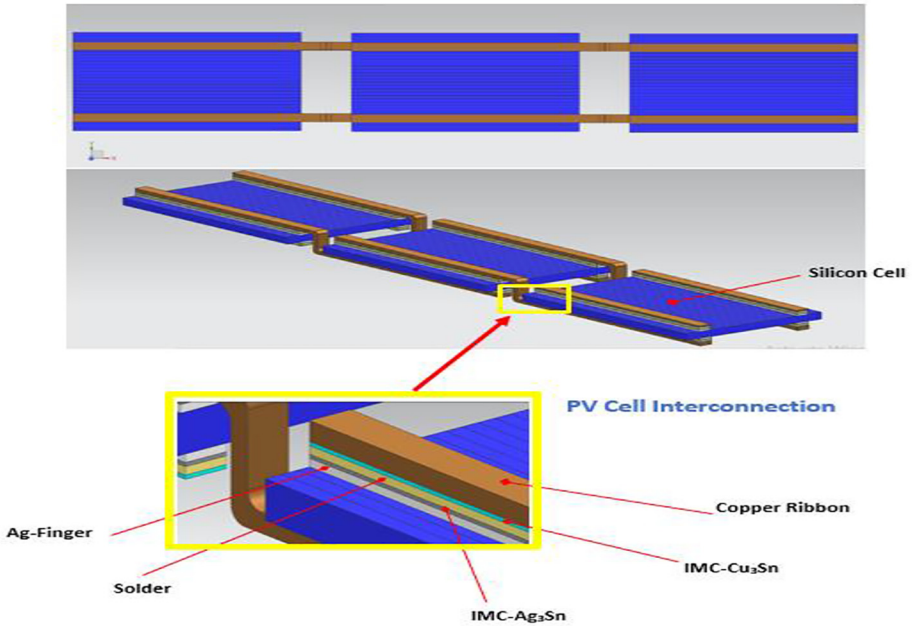

Fig. 1. Conventional front-to-back cell interconnection technology in c-Si PV module.

Please cite this article as: F. K. A. Nyarko, G. Takyi, E. H. Amalu et al., Generating temperature cycle profile from in-situ climatic condition for accurate prediction of thermo-mechanical degradation of c-Si photovoltaic module, Engineering Science and Technology, an International Journal, https://doi.org/10.1016/j.jestch.2018.12.007

induces compressive stresses in the assembly and pushes the cells closer. A number of researchers have made significant contributions to the study of thermal cycling reliability of solder joints. However, the majority of the study focused primarily on flip chip and BGA packages [19–22]. Research into thermal cycling of soldered interconnects in PV modules remain fewer in literature.

This investigation involves a study of in-situ operating module temperature of some field c-Si PV modules. The study uses a three-year data from 2012 to 2014 and develops temperature cycle profile of each year. Consequently, the temperature profiles are used to generate a representative temperature profile for the test region.

2. Experimental methods

Fig. 2 shows the rig for monitoring the outdoor climate used for this study. The rig contains other types of crystalline silicon PV modules. However, only the mono-crystalline that is used for this investigation. Additionally, Fig. 3 presents the sub-station for the data collection. The rigs are located at college of Engineering KNUST, Kumasi, Ghana, West Africa. The system was installed in 2012 with financial assistance from The World Bank through Africa Renewable Energy Access programme (AFREA) under the project title: Capacity Upgrading for West African Partners in Renewable Energy Education. Table 1 lists the system specifications and capacity of the modules. The site location (College of Engineering, KNUST, Kumasi, Ghana) is on latitude 6° 40′ N and longitude 1° 37′ W, at an elevation of 250 m above sea level. The modules are unshaded and mounted on an inclined rooftop with a tilt angle of 5°, and oriented toward the equator (southwards). Furthermore, a 4 kW SMA Sunny Boy DC-AC inverter (SB 3800) connects each of the various PV module technologies to the grid. There are five inverters connected and integrated to communicate with a SMA Sunny WebBox via a Bluetooth ad-hoc connection. Consequently, the SMA Sunny WebBox transmits the data output from the PV systems and stores on a dedicated server. Additionally, an SMA Sunny portal created on the dedicated server from the University network provided an online monitoring system.

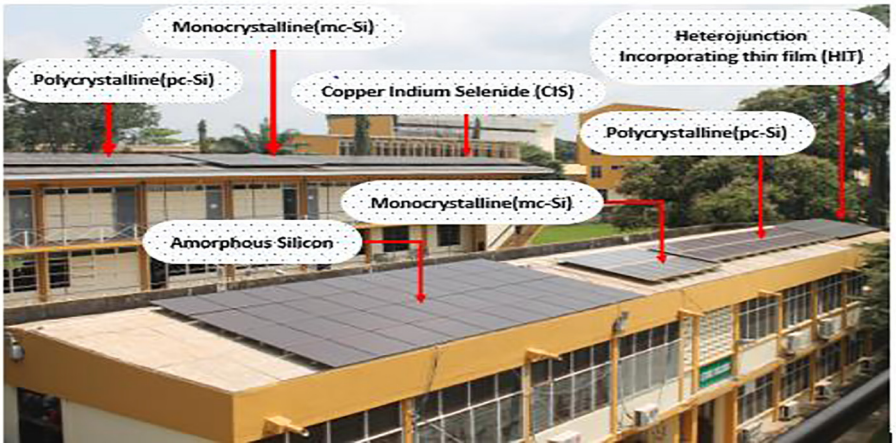

Fig. 2. Outdoor monitoring set-up at college of engineering KNUST, Kumasi, Ghana.

Fig. 3. Monitoring station for outdoor test set-up at college of engineering KNUST, Kumasi, Ghana.

Please cite this article as: F. K. A. Nyarko, G. Takyi, E. H. Amalu et al., Generating temperature cycle profile from in-situ climatic condition for accurate prediction of thermo-mechanical degradation of c-Si photovoltaic module, Engineering Science and Technology, an International Journal, https://doi.org/10.1016/j.jestch.2018.12.007

Table 1
Technical specification of modules in the experiment rig.

Cell Technologies	Amorphous Silicon	Mono-crystalline Silicon	Poly-crystalline Silicon	HIT	Copper Indium disulfide (CIS)
Model × String	10 × 4	7 × 3	9 × 2	8 × 2	9 × 9
Total number of modules	40	21	18	16	81
Power per module (W)	100	190	225	250	50
Total module peak power (W)	4000	3990	4050	4000	4050
Voltage at nominal power (V)	30.7	36.4	29.4	34.9	36.8
Current at nominal power (A)	3.25	5.22	7.55	7.18	1.36
Open circuit voltage (V)	40.9	45.2	36.7	43.1	49.5
Open circuit current (A)	3.85	5.46	8.24	7.74	1.66
Maximum system voltage (V)	1000	1000	1000	1000	1000
Temperature coefficient of open circuit voltage (%/°C)	−0.33	−0.33	−0.33	−0.01	−0.26
Temperature coefficient of short circuit current (%/°C)	0.08	0.03	0.04	0.03	0.04
Temperature coefficient power (%/°C)	−0.20	−0.44	−0.45	−0.30	−0.30
Total surface area of PV system (m^2)	58.9	28.1	30.6	22.6	68.6
Nominal power of PV-module (kW)	4.0	3.99	4.05	4.0	4.05
Module efficiency (%)	6.9	14.5	13.7	18.0	6.1
NOCT	49	46	47.2	46	47

Calibrated platinum sensors (PT100) with measurement accuracy of ±0.5 °C, resolution of 0.1 °C and positioned at the center of each module (on the backside) measured the module temperatures. The data logged included; environment temperature, total insolation, module temperature, operating current and voltage, wind speed and total output power.

3. Results, analysis and discussions

The Sunny Webbox transmits high-resolution data logged at 5 min interval that is logged on a dedicated server from March 2012 to December 2014. The study and data analysis is limited to the monocrystalline PV-modules. This section discusses the observed climatic data and the analysis for the generation of temperature cycle profiles for the three years.

3.1. Daily temperature cycle profile

The data logged at five-minute time interval produces 288 data points every 24 h. Fig. 4 presents the distribution of module temperature signals observed during the study. Fig. 4 shows that the modules recorded relatively higher frequencies of low temperature signals (peaking around 23 °C) for each of the respective years (201–2014). This observation is because the PV modules experience up to about 12 h of lower nighttime temperatures by virtue of geographical location of the test site. As stated earlier, the mod-

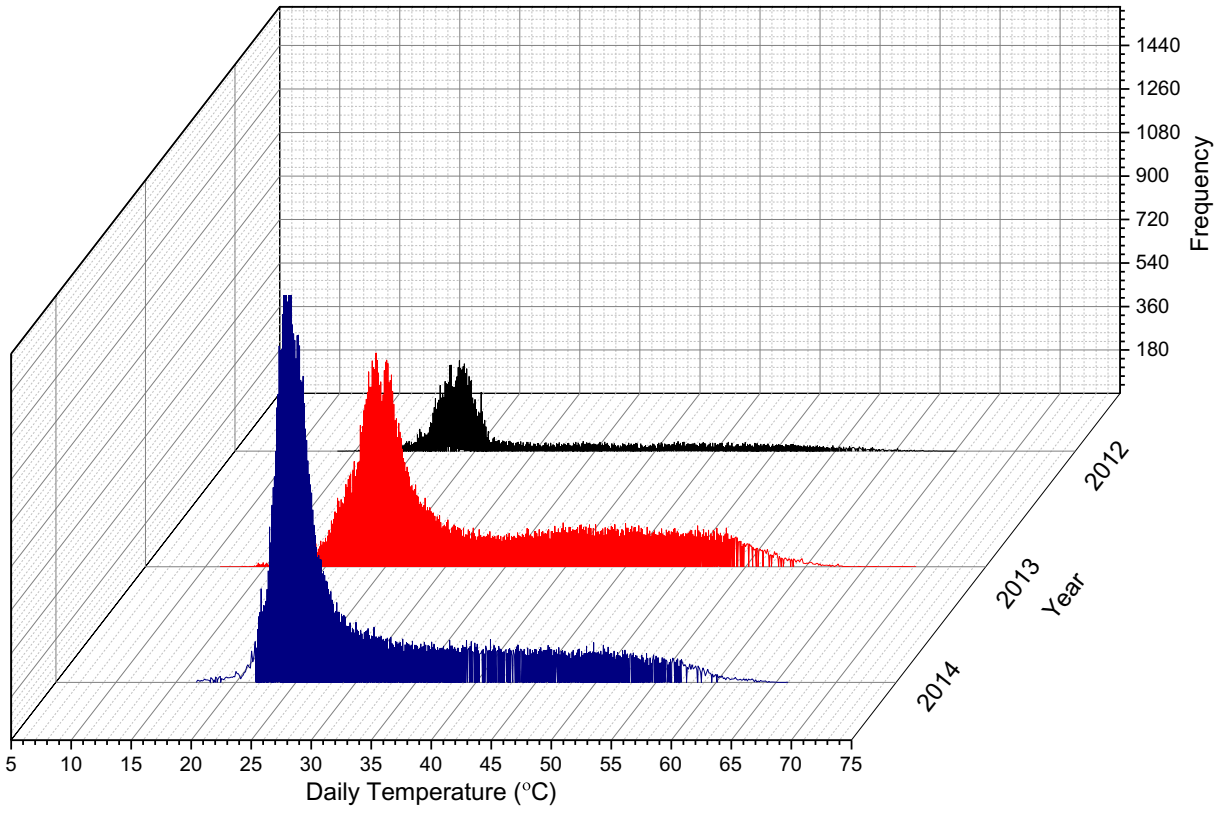

Fig. 4. Distribution of observed daily module temperatures for 2012, 2013 and 2014 years.

Please cite this article as: F. K. A. Nyarko, G. Takyi, E. H. Amalu et al., Generating temperature cycle profile from in-situ climatic condition for accurate prediction of thermo-mechanical degradation of c-Si photovoltaic module, Engineering Science and Technology, an International Journal, https://doi.org/10.1016/j.jestch.2018.12.007

Table 2
Summary of observed daily temperature for years 2012, 2013 and 2014.

Year	2012	2013	2014
Mean (°C)	30.0	31.8	31.9
Minimum (°C)	13.5	11.2	16.7
Maximum (°C)	65.1	69.2	66
Std. Deviation (°C)	10.4	10.6	10.3
Range (°C)	51.6	58	49.3
Skewness	1.01	0.91	1.15

ule temperature data was logged from March 2012. Consequently, the size of the data points generated in 2012 was relatively smaller than that of the years 2013 and 2014. This accounted for the low concentration of temperature signals displayed for the year 2012. We further observed a mild year-to-year variation in temperature distribution between the year 2013 and 2014. The year 2013 recorded slightly higher peaks in temperature signals between 35 °C and 60 °C compared with the year 2014.

Table 2 presents the statistics of some critical indices of the observed daily temperatures. It shows that year 2012 recorded the lowest minimum module temperature of 13.5 °C whereas the year 2013 recorded the maximum module temperature of 69.2 °C. Furthermore, the year 2013 recorded the highest temperature range of 58 °C. The logged data was analyzed further to produce plots of average daily temperature profiles of each month for the three years.

Fig. 5 presents the daily module temperature profiles (monthly average). The figure depicts that the average daily module temperature starts from around 20 °C (midnight at local time, 00:00 hrs) and slightly increases up to about 22 °C at around 06:00 h and peaks around 57 °C at about 12:45 pm local time. Subsequently, the temperature decreases to around 22 °C at about 18:00 pm. Fig. 6 shows that from the months of January to May, year 2013 has highest average daily temperatures while year 2012 has lowest values. Furthermore, it shows that from June to December, year 2012 recorded the highest average daily module temperature while year 2014 recoded the lowest.

3.2. Temperature gradient of thermal cycle profile

The daily temperature gradients of the cyclic temperature profile were determined from the logged module temperatures. The temperature gradients resulted from the difference between the peak daytime temperature and the minimum nighttime temperature. The frequency distribution of the daily temperature gradients present sufficient data to model the temperature cycle of the PV modules for accurate outdoor weathering prediction. Fig. 6 shows the distribution of temperature gradients for the mono c-Si PV module for the years 2012, 2013 and 2014. As observed from Fig. 6, the yearly profiles are relatively similar. The frequency distribution of the observed temperature gradients show curves with spikes, skewed towards higher temperature gradients. The mean temperature gradients of the modules are 38.7 °C, 33.8 °C and 33.6 °C for 2012, 2013 and 2014, respectively. The data compares well with results obtained from similar studies by Herrmann et al. [23].

3.3. Module temperature 'rainflow' counting analysis

Intra-day module temperature fluctuations caused by cloud movements have been demonstrated to have more damaging effect on c-Si PV module compared with day/night temperature gradient [24]. Fig. 6 show all-year round daily temperature. The highly unpredictable nature of cloud cover and subsequent fluctuation of irradiance present great difficulty in characterizing short-time intraday cycles. Cycle counting presents the best approach to stress-load analysis. Furthermore, the rainflow counting algorithm [25] offers the best cycle counting method for effectively compressing a time series data into peaks and valleys. The peaks and valleys in the temperature signal presents reversal points at which half-cycles are determined. The algorithm counts a cycle by considering a moving reference temperature point of the sequence, say 'T_P', and a moving ordered three-temperature point subset T_X and T_Y with the following characteristics:

- The first and second temperature points are collectively named as T_Y
- The second and third temperature points are collectively named as T_X
- The absolute value of the difference between the amplitude of the first and second temperature point is the range of T_X denoted by $r(T_X)$.
- Range of T_Y is also denoted by $r(T_Y)$

Fig. 7 displays the flowchart for the rainflow counting algorithm. The rainflow counting algorithm is generated using a MATLAB program and has been successfully deployed in this work to determine the number of temperature cycles experienced by the modules each year.

Fig. 8 shows temperature cycles counted for the years 2012, 2013 and 2014 using the rainflow algorithm. Fig. 8 reveals that sunrise and sunset ramping events correspond to low-frequency high-temperature range half-cycles. In addition, intra-day temperature fluctuations correspond to short-range high-frequency temperature points. Typically, the tropical climate exhibits short-range high-frequency temperature ramping events mainly due to the presence of cloudy skies. More short-range ramping events were recorded for the year 2013 (28% over 2012) and 2014 (3% over 2012). The results trend closely with similar studies for a tropical climate by Owen-Bellini et al. [14].

3.4. Heating and cooling rates of the module

A PV module ramp rate defines the rate of heating and/or cooling of PV modules subjected to temperature cycle loading. Recently, some PV module test-qualification methods have used higher ramp rates to reduce test time and save resources. The accelerated temperature cycle (ATC) demonstrates the adequacy in modelling the degradation of systems subjected to temperature cycling in the field. However, the determination of accurate ATC model from in-situ climate remains a challenge. The accurate determination of the magnitude of the ramp rate is critical in producing the correct ATC profile. More so as its effect on thermo-mechanical degradation of PV modules. The relationships between ramp rate and the various degradation mechanisms such as thermally induced expansion and contraction of various elements within the module and interconnect present a key research outcome. There is also, highly accelerated temperature cycle (HATC) test technique among others.

In this study, the heating and cooling rates of the monocrystalline silicon PV module are evaluated and analyzed using the IBM SPSS analysis tool [26]. Figs. 9 and 10 show the distribution of ramp rates obtained from the analyses of the data logged. The cumulative duration on the vertical axis evaluates the total time the PV module recorded a particular cooling/heating rate. From Fig. 9, the majority of ramp rates are well below 50 °C/h. Though there are ramp rates up and above IEC 61215-test rate of 100 °C/h, the frequencies of their occurrence are relatively lower. Table 3 presents a summary of ramp rates recorded by modules for each test year. The mean ramp rates are very low – below 11 °C/h for all the years. However, Table 3 depicts occurrences of higher heat-

Please cite this article as: F. K. A. Nyarko, G. Takyi, E. H. Amalu et al., Generating temperature cycle profile from in-situ climatic condition for accurate prediction of thermo-mechanical degradation of c-Si photovoltaic module, Engineering Science and Technology, an International Journal, https://doi.org/10.1016/j.jestch.2018.12.007

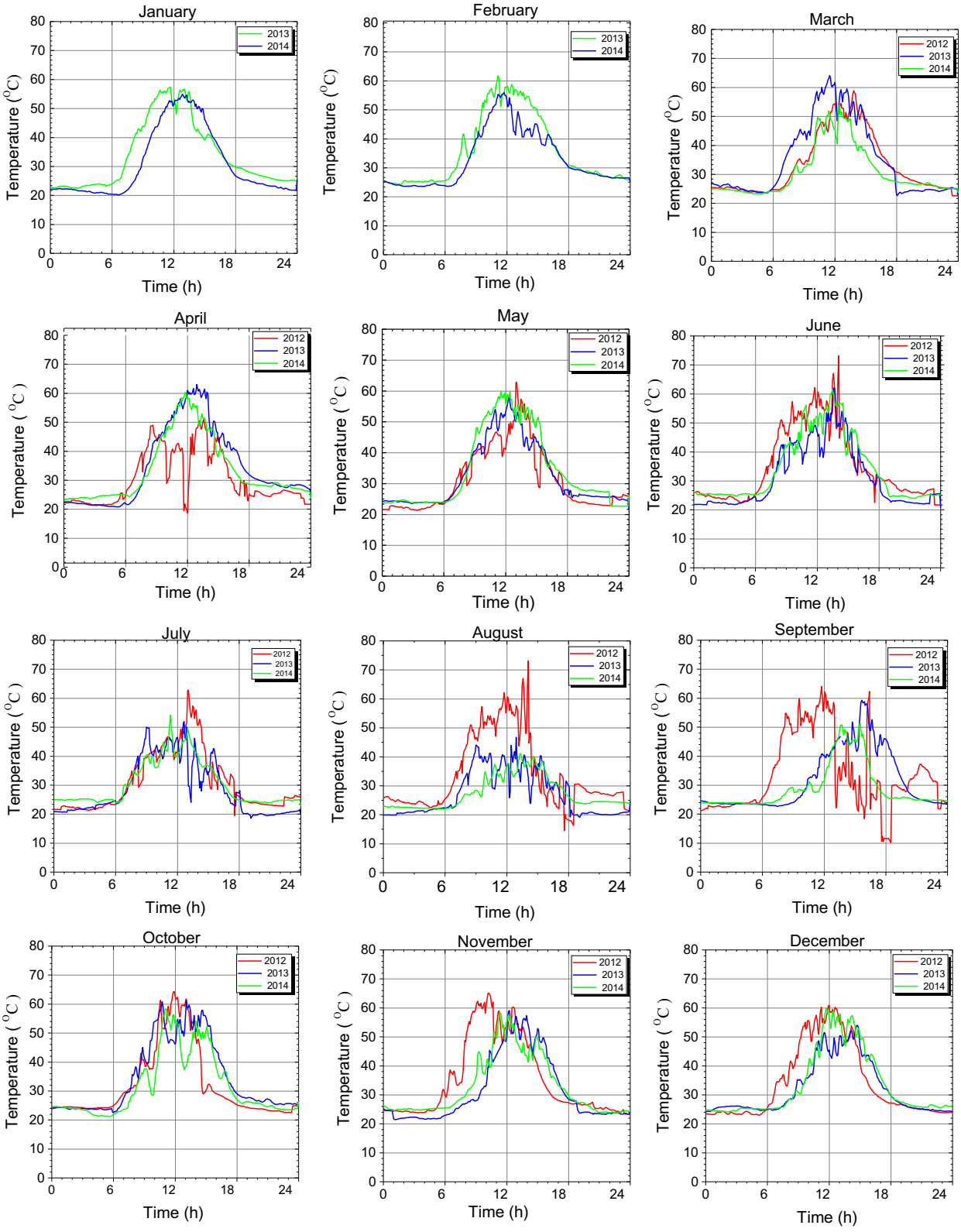

Fig. 5. Daily temperature profile (monthly average) observed for 2012–2014.

ing and cooling rates that are three times higher than the IEC 61215-test rate. Table 3 further reveals percentage increase in maximum ramp rates of 238%, 147%, and 228% over the IEC 61215-ramp rate for years 2012, 2013 and 2014, respectively. The statistics are quiet significant considering that higher heating and cooling rates increase the damage accumulation that subsequently accelerate degradation of soldered joints of the PV module [27].

Please cite this article as: F. K. A. Nyarko, G. Takyi, E. H. Amalu et al., Generating temperature cycle profile from in-situ climatic condition for accurate prediction of thermo-mechanical degradation of c-Si photovoltaic module, Engineering Science and Technology, an International Journal, https://doi.org/10.1016/j.jestch.2018.12.007

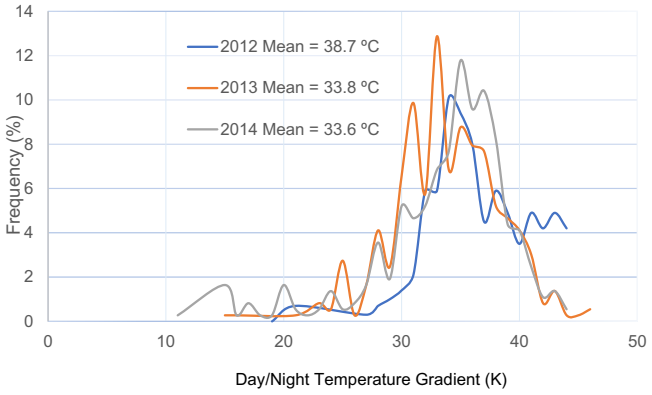

Fig. 6. Frequency distribution of daily module temperature (monthly average) gradients observed for 2012–2014 at test site.

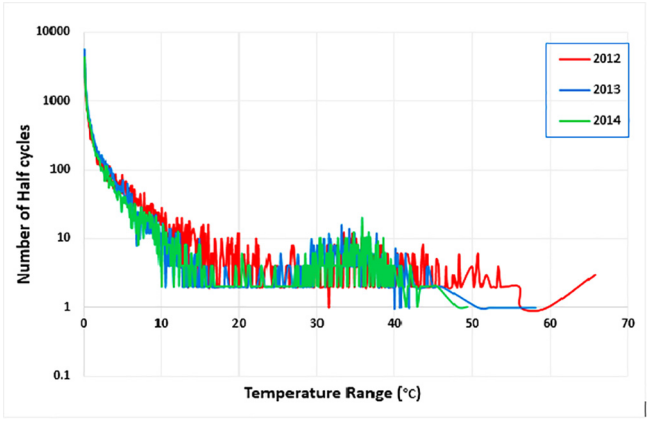

Fig. 8. Distribution of cycles counted for each year (2012–2014).

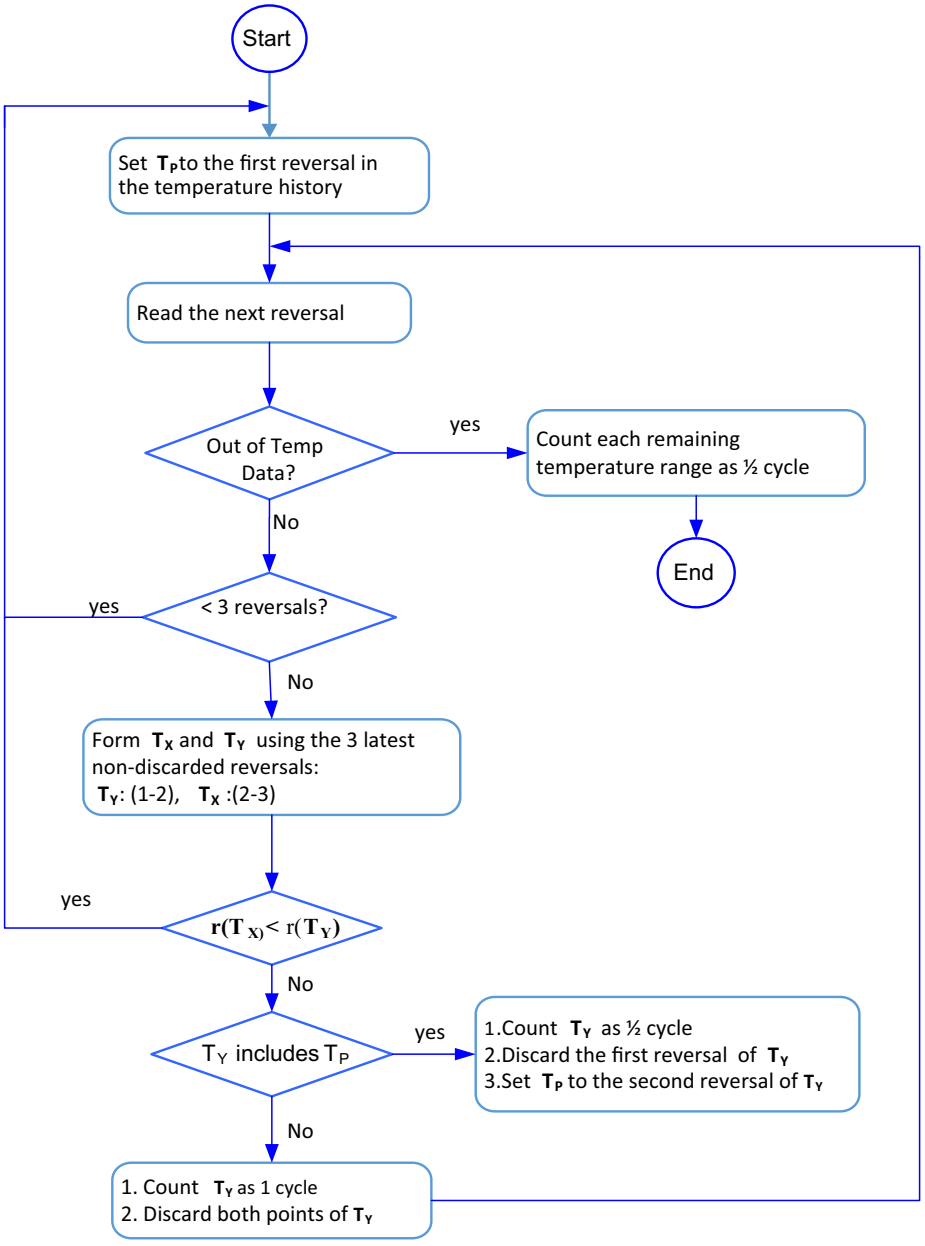

Fig. 7. Flowchart for rainflow counting.

Please cite this article as: F. K. A. Nyarko, G. Takyi, E. H. Amalu et al., Generating temperature cycle profile from in-situ climatic condition for accurate prediction of thermo-mechanical degradation of c-Si photovoltaic module, Engineering Science and Technology, an International Journal, https://doi.org/10.1016/j.jestch.2018.12.007

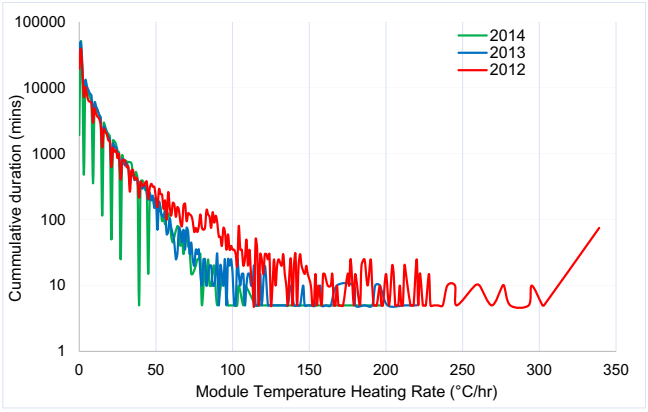

Fig. 9. Cumulative frequency distribution of observed heating rates at test site.

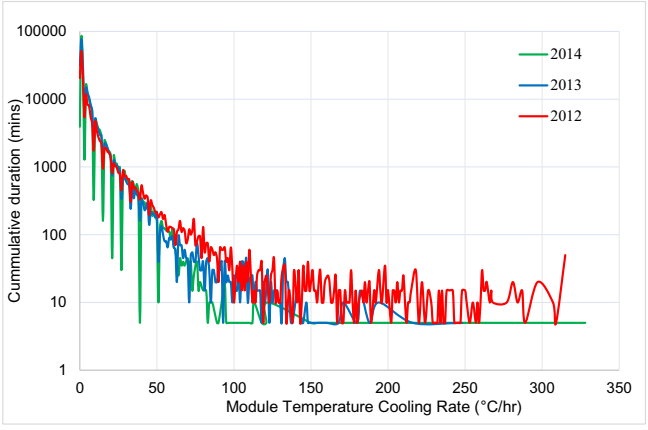

Fig. 10. Cumulative frequency distribution of observed cooling rates from 2012 to 2014.

Table 3
Summary of observed heating and cooling rates and maximum ramp rates.

Year	2012	2013	2014
Heating rates			
Mean (°C/h)	8.58	7.1	7.56
Maximum (°C/h)	339	220	198
% increase from IEC 61215 (100 °C/h)	238	120	98
Cooling rates			
Mean (°C/h)	10.44	10.2	10.1
Maximum (°C/h)	315	248	328
% increase from IEC 61215 (100 °C/h)	215	148	228
Maximum ramp rates			
Maximum heating rates (°C/h)	339	220	198
Maximum cooling rates (°C/h)	315	248	328
Maximum ramp rate (°C/h)	339	248	328
Maximum ramp rate (°C/min)	5.65	4.13	5.46
% increase from IEC 61215 (1.67 °C/min)	238%	147%	228%

3.5. Temperature dwell times of the PV module

Theoretically, the temperature dwell time for a PV module is the time the module records a zero temperature ramp. It is the time the module is soaked at a constant temperature. There are two main dwell times in a daily temperature cycle. The upper and lower dwells corresponding to the upper and lower temperature regimes. The plots of daily module temperature cycles presented in Fig. 5 assist in the estimation of dwell times in the module temperature cycle. In this study, a module assumes a temperature

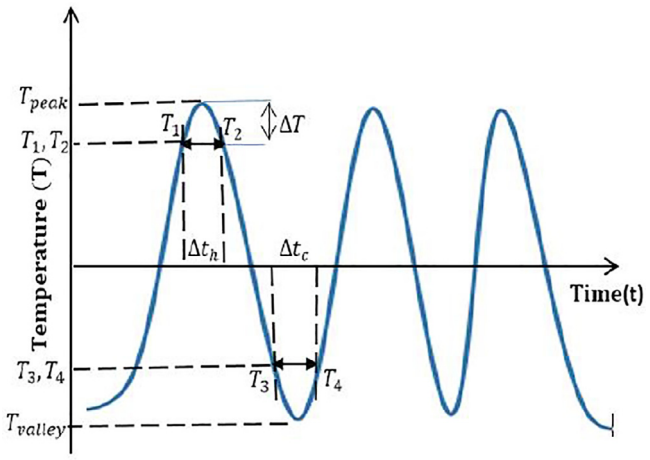

Fig. 11. Typical temperature cycle.

dwell if the rate of temperature rise in an interval is lower than the mean ramp rate. Fig. 11 helps to illustrate how to compute a dwell time from a typical temperature cycle with peak and valley temperatures.

The analysis for evaluating the dwell times are as follows:

$$\Delta T = mean\ ramp\ rate\ \left(\hat{A}^{\circ}C/min\right) \times (temperature\ signal\ time\ interval\ (min)) \quad (1)$$

The conditions for computing hot dwell time range (Δt_h) require that:

$$T_{peak} - T_1 \leq \Delta T \quad (2)$$

$$T_{peak} - T_2 \leq \Delta T \quad (3)$$

Similarly, conditions for computing cold dwell time range (Δt_c) require that;

$$T_3 - T_{valley} \leq \Delta T \quad (4)$$

$$T_4 - T_{valley} \leq \Delta T \quad (5)$$

For instance, in the year 2012 the mean heating rate observed is 8.85 °C/hr (0.14 °C/min). Thus in five minutes the module temperature rises by a mean value of 0.7 °C ($\Delta T = 0.7\hat{A}^{\circ}C$). Therefore, the time range for temperatures on either side of the peak temperature which are less than the peak temperature by 0.7 °C is considered as the upper (also known as hot) dwell time for the cycle. Similarly, a lower (also known as cold dwell) dwell time is the time range for temperatures on either side of the lowest temperature that are more than the lowest temperature by 0.7 °C. The authors replicated the analysis for the data for years 2013 and 2014 to compute their respective dwell times. The huge size of the temperature data logged required an algorithm that could pick out the temperatures around the peaks and valleys and subsequently compute the dwell times. Fig. 12(a) and (b) show flowcharts of MATLAB algorithms used in computing the dwell times.

Figs. 13 and 14 present a monthly average distribution of the dwell times (hot and cold) generated with the MATLAB algorithm. Table 4 lists the yearly average distribution of the hot and cold dwell times.

From Figs. 13, 14 and Table 4 the cold dwell time remain constant averaging between 359-to-390 min with fewer spikes up to a maximum of 510 min. In Table 4, the year 2014 recorded the highest cold dwell times of 510 min, whilst year 2012 recorded

Please cite this article as: F. K. A. Nyarko, G. Takyi, E. H. Amalu et al., Generating temperature cycle profile from in-situ climatic condition for accurate prediction of thermo-mechanical degradation of c-Si photovoltaic module, Engineering Science and Technology, an International Journal, https://doi.org/10.1016/j.jestch.2018.12.007

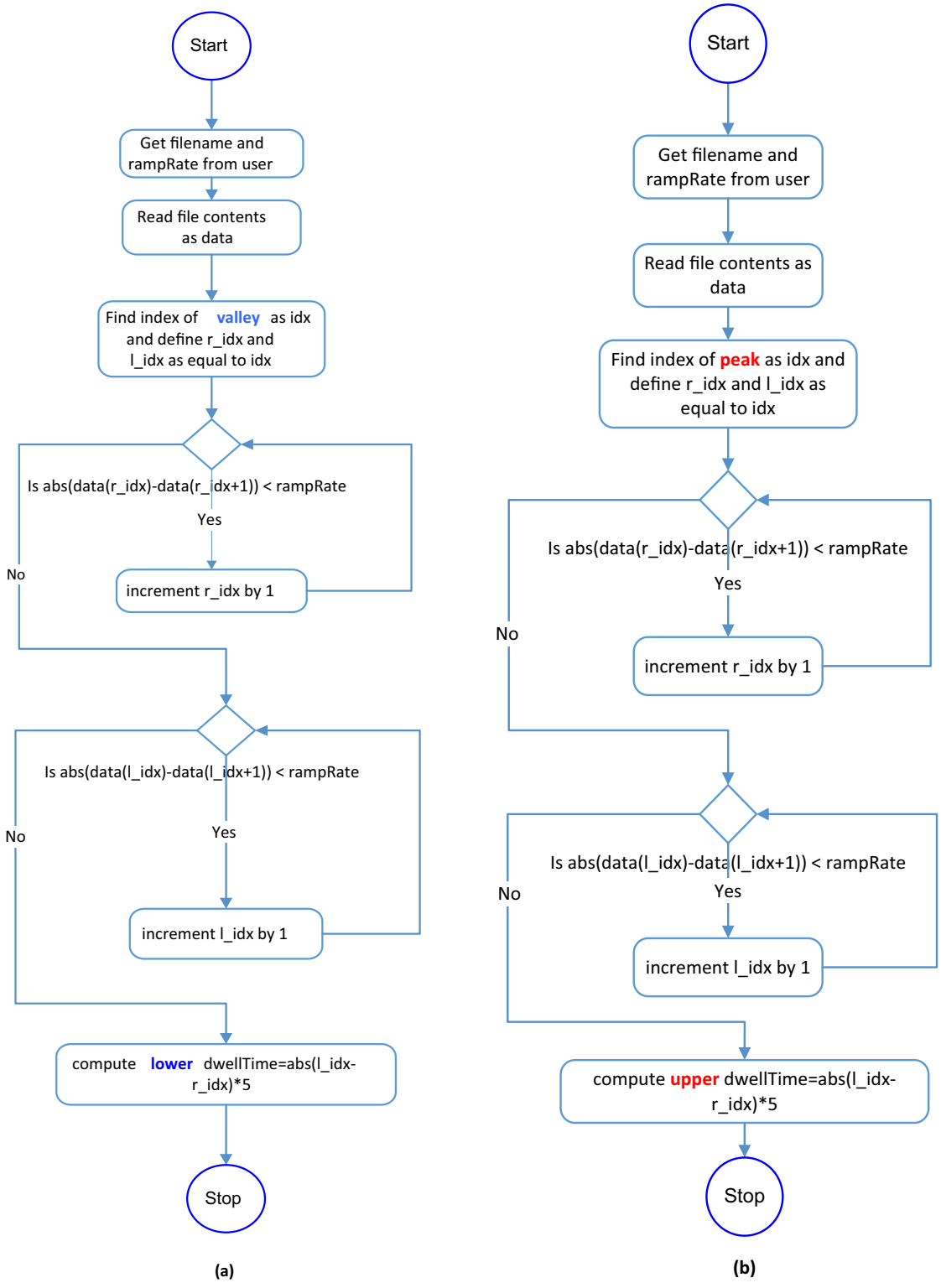

Fig. 12. Flowchart for computing dwell times; (a) lower dwell (b) upper dwell.

the highest hot dwell time of 435 min. The observed average hot and cold dwell times for the respective test years are far in excess of the 10-minute dwell time for IEC 61,215 test cycle. This is because modules maintain near constant peak temperatures for about three hours during the day, and maintain a near constant temperature over long periods (over 6 h) upon cooling at night.

3.6. Generating in-situ temperature cycle (ATC) profile using the data logs

Electronic assembling and packaging industries have successfully used Accelerated temperature cycle (ATC) profiles to assess thermo-mechanical reliability of microelectronic devices. The

Please cite this article as: F. K. A. Nyarko, G. Takyi, E. H. Amalu et al., Generating temperature cycle profile from in-situ climatic condition for accurate prediction of thermo-mechanical degradation of c-Si photovoltaic module, Engineering Science and Technology, an International Journal, https://doi.org/10.1016/j.jestch.2018.12.007

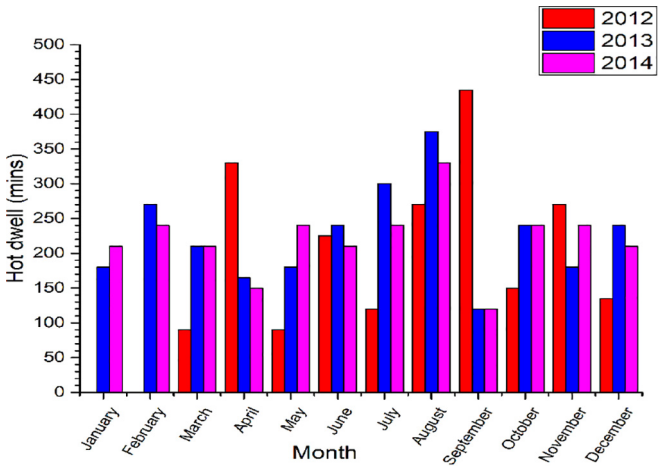

Fig. 13. Monthly average distribution of hot dwell times (2012–2014).

method reduces product test time and maximizes resource usage. Depending on experimental designs, the procedure may involve: increasing the applied temperature range, heating and cooling rates or decreasing temperature dwell times [28]. The relative impact of these cycle parameters in terms of the damage induced on interconnections of assemblies remain under research. The impact of heating and cooling rates also remain uncertain.

This study uses the mean values of the ramp rates, dwell times, maximum and minimum temperatures experienced by the module in each of the respective years to generate in-situ temperature cycle profile representative of the test region. Table 4 presents a summary of the values of the critical parameters used to plot each temperature cycle profile of the years and the IEC 61215 condition. Fig. 15 shows the actual daily temperature profiles recorded and fitted with a representative thermal cycle profiles for the respective years (2012–2014). The profiles show extended dwell times as well as overall cycle time. A typical daily cycle time completes in 86,400 s (24 h). As shown from Table 4, the mean daily temperature gradients for the generated cycles are relatively smaller when compared with the IEC 61215. A maximum of 40.2 °C recorded in 2012 whereas the IEC 61215 temperature gradient is 125 °C. The summary of the critical parameters presented in Table 4 shows that the effect of employment of IEC 61215 test on thermo-mechanical degradation qualification of c-Si PV module is likely to be significantly different from the generated temperature cycles.

For critical comparison, we combine the temperature profiles (2012–2014) and denote as Test Region Average (TRA) cycle. Section 3.7 discusses the TRA cycle and the IEC 61215 cycle.

3.7. Comparison of critical parameters of the generated ATC profile for test region with IEC 61215 test qualification

This section presents an ATC profile proposed to be representative for the test site. This is achieved by averaging the various cycle parameters such as the ramp rates, dwell times (Hot and Cold dwell), minimum module temperatures and maximum module temperatures. The section also discusses the critical parameters such as cycle time, ramp rates, dwell times and temperature gradients. Table 5

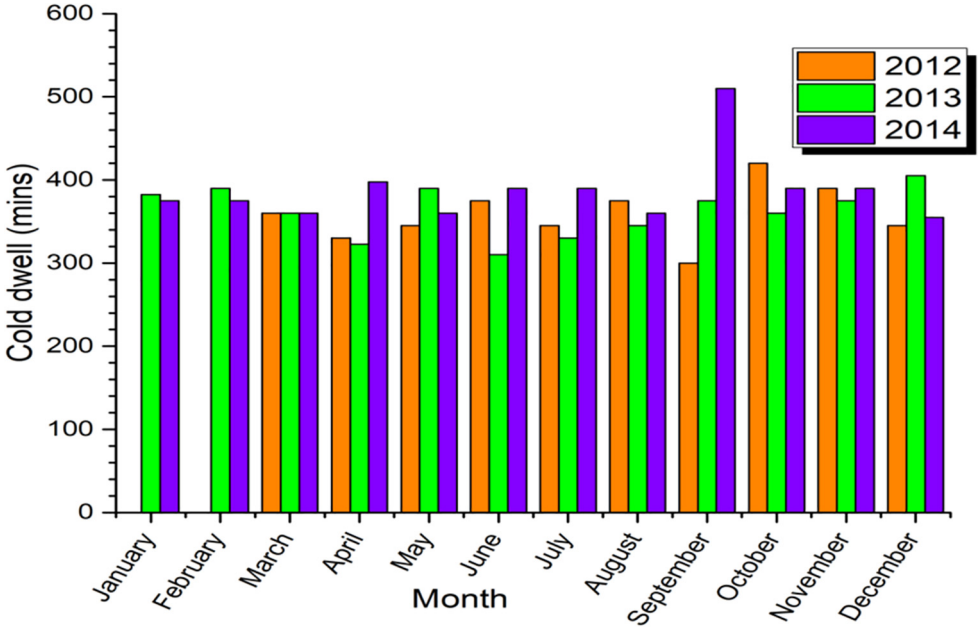

Fig. 14. Monthly average distribution of cold dwell times (2012–2014).

Table 4
Summary of the parameters of the temperature cycle profile of the years.

Test Year		2012	2013	2014	IEC 61215
Dwell time (min)	Mean Hot dwell	212	225	219	10
	Mean Cold dwell	359	357	390	10
Ramp rate (°C/h)	Mean. ramp rate	9.51	8.65	8.82	100
Mean module Hot Dwell Temperature (HDT)/(°C)		63.7	57.9	56.1	85
Mean module Cold Dwell Temperature (CDT)/(°C)		23.5	23	24.4	−40
Temperature gradient (°C)		40.2	34.9	31.7	125

Please cite this article as: F. K. A. Nyarko, G. Takyi, E. H. Amalu et al., Generating temperature cycle profile from in-situ climatic condition for accurate prediction of thermo-mechanical degradation of c-Si photovoltaic module, Engineering Science and Technology, an International Journal, https://doi.org/10.1016/j.jestch.2018.12.007

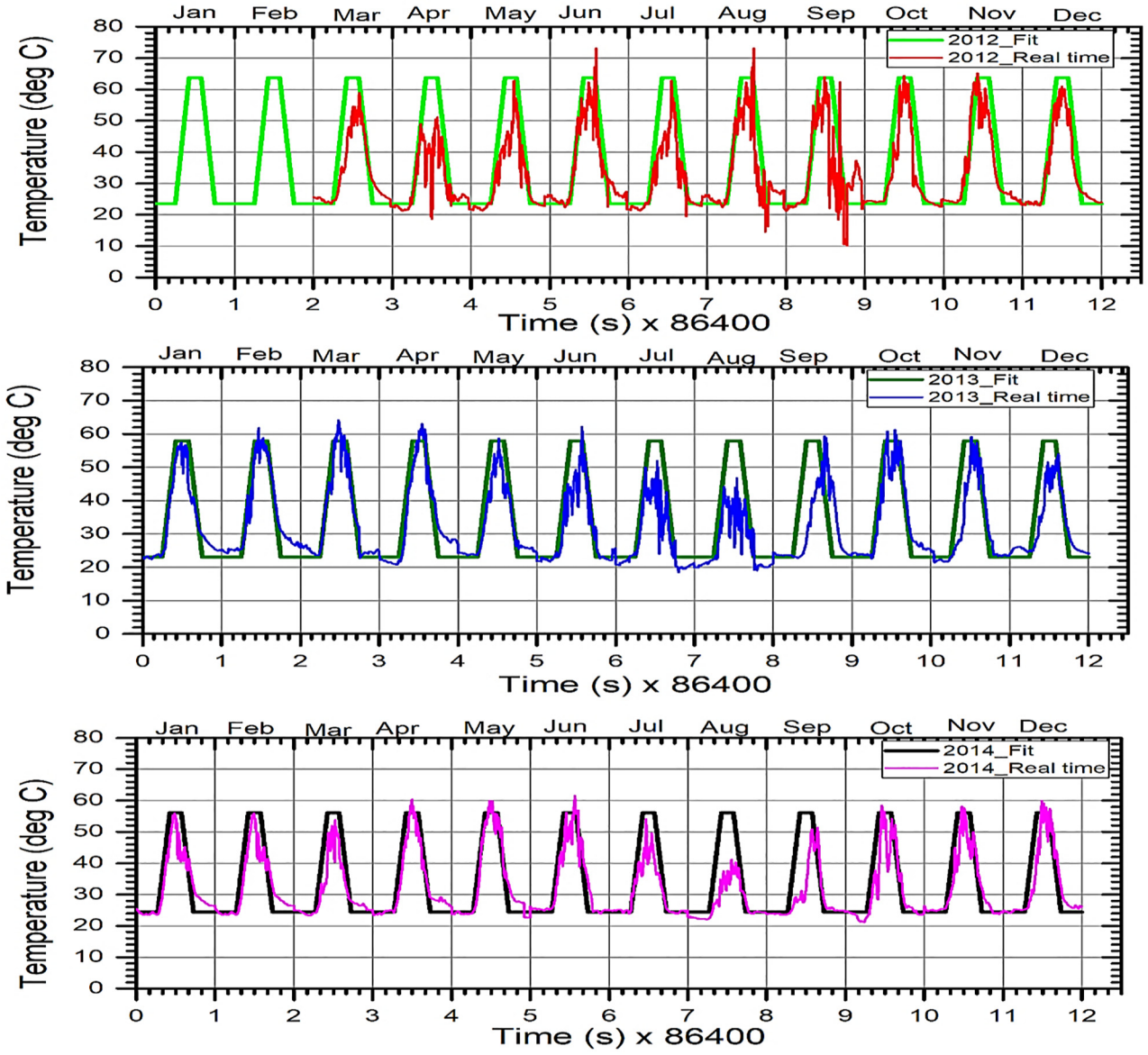

Fig. 15. In-situ thermal cycle profiles fitted onto real time module temperature profile for 2012–2014.

Table 5
Summary of ATC profile parameters for Test Region and IEC 61215.

ATC Profiles	Ramp Rates (°C/h)	Dwell Times (min)		Maximum Temperature (°C)	Minimum Temperature (°C)	Temperature Gradient (°C)
		Hot	Cold			
Test Region Average (TRA)	8.996	228	369	58.9	23.7	35.2
IEC 61215	100	10	10	85	−40	125
% Difference	−91%	2180%	3590%	−30.7%	−159.3%	−71.8%

presents the data analysis. Fig. 16 (a) and (b) display the IEC 61215 profile and the generated TRA thermal cycle profile respectively. In general, the IEC 61215 features a relatively higher ramp rate of 100 °C/h, shorter dwell time, short cycle time (10200 s) and a higher temperature gradient. The generated TRA profile on the other hand, has relatively lower average ramp rates of 8.996 °C/h, longer cold and hot dwell time, longer cycle time (86400 s) and lower temperature gradient.

3.7.1. Ramp rate

Table 5 shows that the ramp rate for the test region and the IEC 61215 are 8.996 °C/h and 100 °C/h, respectively. The statistics demonstrates that the ramp rate of test region (TRA) is 91% at variance with the ramp rate for IEC 61215-test cycle. A slower ramp rate leads to longer cycle time. The phenomenon accounts for the long completion of temperature cycle of in the sub-Saharan African TRA cycle.

It is reported that cyclic strain energy increases with slower ramp rates in Pb-free (SAC) solder joints in chip resistor assemblies [29]. The assertion is supported by a similar research [30] which concluded that thermal cycling with slower ramp rates lead to largest reduction in shear strength. However, the results for tin-lead (PbSn) solder alloys appear to be on the contrary. For SnPb solders, results from studies conducted in [30,31] predicted a decrease in

Please cite this article as: F. K. A. Nyarko, G. Takyi, E. H. Amalu et al., Generating temperature cycle profile from in-situ climatic condition for accurate prediction of thermo-mechanical degradation of c-Si photovoltaic module, Engineering Science and Technology, an International Journal, https://doi.org/10.1016/j.jestch.2018.12.007

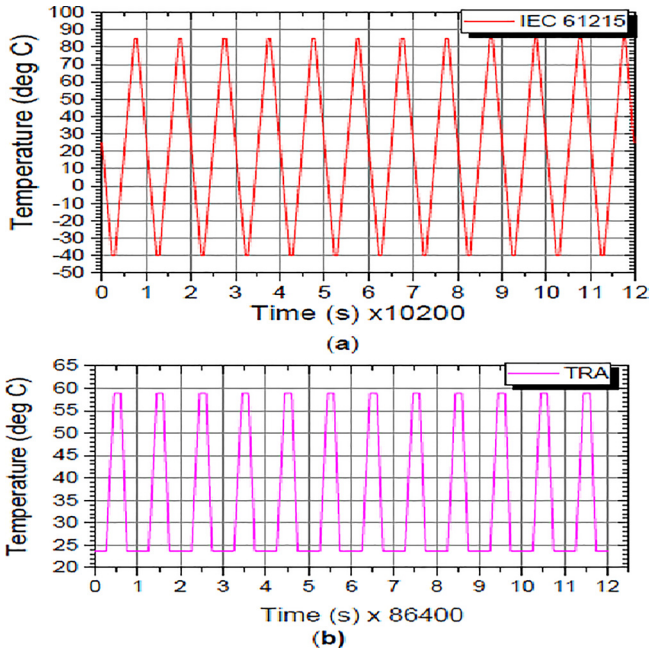

Fig. 16. Plots of twelve-cycle profile of (a) the IEC 61215 test qualification and (b) the test region average (TRA).

cyclic life with increasing ramp rates. Generally, short temperature cycle time accelerates the damage of the interconnection in the c-Si PV module by inducing a thermal shock in the system. It is significant to note that these studies reported on the solder joint lives in chip resistor assemblies. The current authors are yet to identify results from studies on effects of ramp rates on solder interconnections in c-Si PV module in the literature.

3.7.2. Dwell time

From Table 5 the hot and cold dwell times of the generated single cycle of the test region TRA are excessively higher than the IEC 61215. For instance, the hot dwell time of the test region is 2180% at variance with the IEC 61215 dwell time. The difference in dwell time could have adverse impact on the Mean Time to Failure (MTTF) of the c-Si PV module operating in the sub-Saharan Africa test site. Many studies conducted on eutectic solder joints reported that the dwell time beyond certain limit has a minimal effect on the MTTF [31–33].Thus additional increase in dwell time will not produce additional damage beyond a certain limit. Other results show that due to rapid stress relaxation at the maximum cycle temperature, increasing the dwell time at high temperature produces little effect in creep damage of solder joints [34]. However, the authors in [34] observed a reduction in fatigue life due to increased creep strains at increased cold dwell time. Syed [35] reported that a longer dwell time causes more accumulated creep damage in the solder joint – thus lowering the fatigue life significantly. It is therefore important to study the impact of dwell times on thermo-mechanical reliability of soldered interconnections in c-Si PV modules.

3.7.3. Temperature gradient and temperature cycle boundary conditions

Data from Table 5 shows that the profiles have average maximum module temperatures of 58.9 °C and 85 °C for the Test Region and the IEC 61215, respectively. The test region recorded an average minimum temperature of 23.7 °C whereas the IEC 61215 cycle has a minimum temperature ramp of −40 °C. The resulting temperature gradient of the test region is 35.2 °C. The value is lower than the IEC 61215 temperature gradient by about 71.8%. Pang et al. [36] reported an increase in accumulated creep strain range experienced by solder joints increases with temperature gradient.

The increase leads to a decrease in the predicted fatigue life. The authors [36] further reported that creep exposure is greater for a higher temperature limit compared with a relatively lower temperature limit. These findings necessitate a critical investigation on the effect of these variables on the interconnect fatigue life of c-Si PV modules.

4. Conclusions

This study analyzed in-situ module temperature history of monocrystalline silicon photovoltaic (c-Si PV) module operating in a sub-Sahara African climate. The temperature history consisted of a three-year observation spanning from 2012 to 2014.

Analysis of the data yields a temperature cycle profile for the test site denoted as TRA cycle. The study proposes TRA cycle as a representative cycle of the sub-Sahara African test site. The generated TRA cycle has magnitudes of the critical parameters of ramp rate, hot and cold dwell times, maximum and minimum temperatures of 8.996 °C/h, 228 min (hot dwell), 369 min (cold dwell), 58.9 °C and 23.7 °C, respectively. The percentage differences between the values of these parameters and the values of corresponding parameters of the IEC 61215 standards for terrestrial PV modules qualification are −91%, 2180%, 3590%, −30.7%, −159.3%, −71.8%, respectively. Furthermore, the percentage difference of the generated cycle time from the IEC61215 cycle time is about 747% (86400 s versus 10200 s). These differences are huge and could explain the high failure rate of c-Si PV modules exhibit during operation in the sub-Sahara Africa region.

The authors propose that the TRA cycle, which is location dependent, be used in finite element modelling of the PV system to predict thermo-mechanical degradation of soldered interconnects at test site. This is necessary to quantify the differences in the rates of thermo-mechanical degradation in the region accurately. Results of the modelling will provide new knowledge to improve the reliability and increase the mean-time-to-failure of the PV modules operating in the region.

Acknowledgement

The authors acknowledge the financial support received from the USAID for the PRESSA project Sub-Grant no. 2000004829 through the US National Academy of Sciences. The authors appreciate the technical support provided by Dr. Mani and Sai Tatapudi at Arizona State University Photovoltaic Reliability Laboratory. The authors also acknowledge the support received from the Norwegian Programme for Capacity Development in Higher Education and Research for Development within the Fields of Energy and Petroleum (EnPE).

References

[1] A.F.Z.D.P. Dumbleton, Photovoltaic Module Weather Durability & Reliability Testing. White Paper 2012; Available from: http://solardurability.com/filestore/186/atlas25plus_whitepaper_final30.pdf.
[2] A.L. Rosenthal, M.G. Thomas, S.J. Durand, A ten year review of performance of photovoltaic systems, in: Photovoltaic Specialists Conference, 1993, Conference Record of the Twenty Third IEEE. 1993.
[3] B. Sørensen, G. Watt, Trends in photovoltaic applications, Survey report of selected IEA countries between 1992 and 2005. 2006.
[4] C. Ike, The effect of temperature on the performance of a photovoltaic solar system in Eastern Nigeria, Res. Inven.: Int. J. Eng. Sci. 3 (2013) 10–14.
[5] T.M. Walsh et al., Singapore modules-optimised PV modules for the tropics, Energy Procedia 15 (2012) 388–395.
[6] O.O. Ogbomo et al., Effect of operating temperature on degradation of solder joints in crystalline silicon photovoltaic modules for improved reliability in hot climates, Solar Energy 170 (2018) 682–693.
[7] P.G. McCormick, H. Suehrcke, The effect of intermittent solar radiation on the performance of PV systems, Solar Energy 171 (2018) 667–674.

Please cite this article as: F. K. A. Nyarko, G. Takyi, E. H. Amalu et al., Generating temperature cycle profile from in-situ climatic condition for accurate prediction of thermo-mechanical degradation of c-Si photovoltaic module, Engineering Science and Technology, an International Journal, https://doi.org/10.1016/j.jestch.2018.12.007

[8] M. Jamaly, J. Kleissl, Spatiotemporal interpolation and forecast of irradiance data using Kriging, Solar Energy 158 (2017) 407–423.
[9] M. Jamaly, J. Kleissl, Robust cloud motion estimation by spatio-temporal correlation analysis of irradiance data, Solar Energy 159 (2018) 306–317.
[10] R.H. Almeida, L. Narvarte, E. Lorenzo, PV arrays with delta structures for constant irradiance daily profiles, Solar Energy 171 (2018) 23–30.
[11] E. Anguera, C.A. Estrada, A new approach for evaluating flux uniformity for dense array concentrator photovoltaic cells, Solar Energy 171 (2018) 330–342.
[12] V. Bone et al., Intra-hour direct normal irradiance forecasting through adaptive clear-sky modelling and cloud tracking, Solar Energy 159 (2018) 852–867.
[13] N.T. Macben Makenzi, Mutua Benedict, Ismael Abisai, Degradation prevalence study of field-aged photovoltaic modules operating under Kenyan climatic conditions, Sci. J. Energy Eng. 3 (2015) 1–5.
[14] M. Owen-Bellini et al., Environmental stress potentials of different climatic regions, in: Proc. 31st European PV Solar Energy Conference, 2015.
[15] G. Cuddalorepatta et al., Durability of Pb-free solder between copper interconnect and silicon in photovoltaic cells, Prog. Photovoltaics: Res. Appl. 18 (3) (2010) 168–182.
[16] N. Park, J. Jeong, C. Han, Estimation of the degradation rate of multi-crystalline silicon photovoltaic module under thermal cycling stress, Microelectron. Reliability 54 (8) (2014) 1562–1566.
[17] S.R. Wenham, M.A. Green, M.E. Watt, Applied Photovoltaics, Center for Photovoltaic Devices and Systems, University of New South Wales, Sydney, Australia, 1994.
[18] M. Gonzalez et al., Thermo-mechanical challenges of advanced solar cell modules, in: Thermal, Mechanical and Multi-Physics Simulation and Experiments in Microelectronics and Microsystems (EuroSimE), 2011 12th International Conference on. 2011.
[19] L. Zhang et al., Reliability behavior of lead-free solder joints in electronic components, J. Mater. Sci.: Mater. Electron. 24 (1) (2013) 172–190.
[20] Y. Zhang et al., The effects of aging temperature on SAC solder joint material behavior and reliability, in: 2008 58th Electronic Components and Technology Conference, 2008, IEEE.
[21] J.H. Pang, T.-I. Tan, S. Sitaraman, Thermo-mechanical analysis of solder joint fatigue and creep in a flip chip on board package subjected to temperature cycling loading, in: Electronic Components & Technology Conference, 1998. 48th IEEE. 1998. IEEE.
[22] F. Che, J.H. Pang, Fatigue reliability analysis of Sn–Ag–Cu solder joints subject to thermal cycling, IEEE Trans. Device Mater. Reliability 13 (1) (2013) 36–49.
[23] W. Herrmann et al. PV module degradation caused by thermomechanical stress: real impacts of outdoor weathering versus accelerated testing in the laboratory, 2010.
[24] N. Bosco, S. Kurtz, Quantifying the Weather: an analysis for thermal fatigue, in: Proceedings of the PV Module Reliability Workshop, Golden, CO. 2010.
[25] M. Musallam, C.M. Johnson, An efficient implementation of the rainflow counting algorithm for life consumption estimation, IEEE Trans. Reliability 61 (4) (2012) 978–986.
[26] IBM. [cited, October 20th]; Available from: https://www.ibm.com/analytics/spss-statistics-software.
[27] A. Skoczek, T. Sample, E.D. Dunlop, The results of performance measurements of field-aged crystalline silicon photovoltaic modules, Prog. Photovoltaics: Res. Appl. 17 (4) (2009) 227–240.
[28] Y. Qi et al., Temperature profile effects in accelerated thermal cycling of SnPb and Pb-free solder joints, Microelectron. Reliability 46 (2–4) (2006) 574–588.
[29] S. Yoon et al., Effect of stress relaxation on board level reliability of Sn based Pb-free solders, in: Proceedings Electronic Components and Technology, 2005. ECTC '05, 2005.
[30] J.-P. Clech, Acceleration factors and thermal cycling test efficiency for lead-free Sn-Ag-Cu assemblies, in: Proceedings, SMTA International Conference, Chicago, IL, 2005.
[31] P. Sharma, A. Dasgupta, Micro-mechanics of creep-fatigue damage in Pb-Sn solder due to thermal cycling—Part II: Mechanistic insights and cyclic durability predictions from monotonic data, J. Electron. Packaging 124 (3) (2002) 298–304.
[32] M. Amagai, Chip Scale Package (CSP) solder joint reliability and modeling, Microelectron. Reliability 39 (4) (1999) 463–477.
[33] C.J. Zhai, Sidharth, R. Blish, Board level solder reliability versus ramp rate and dwell time during temperature cycling, IEEE Trans. Device Mater. Reliability 3 (4) (2003) 207–212.
[34] A. Schubert et al. Reliability assessment of flip-chip assemblies with lead-free solder joints, in: 52nd Electronic Components and Technology Conference 2002. (Cat. No. 02CH37345), 2002.
[35] A. Syed, Predicting solder joint reliability for thermal, power, and bend cycle within 25% accuracy, in: 2001 Proceedings. 51st Electronic Components and Technology Conference (Cat. No.01CH37220), 2001.
[36] J.H.L. Pang, D.Y.R. Chong, T.H. Low, Thermal cycling analysis of flip-chip solder joint reliability, IEEE Trans. Components Packaging Technol. 24 (4) (2001) 705–712.

Please cite this article as: F. K. A. Nyarko, G. Takyi, E. H. Amalu et al., Generating temperature cycle profile from in-situ climatic condition for accurate prediction of thermo-mechanical degradation of c-Si photovoltaic module, Engineering Science and Technology, an International Journal, https://doi.org/10.1016/j.jestch.2018.12.007